

We are IntechOpen, the world's leading publisher of Open Access books Built by scientists, for scientists

6,900

Open access books available

186,000

International authors and editors

200M

Downloads

Our authors are among the

154

Countries delivered to

TOP 1%

most cited scientists

12.2%

Contributors from top 500 universities



WEB OF SCIENCE™

Selection of our books indexed in the Book Citation Index
in Web of Science™ Core Collection (BKCI)

Interested in publishing with us?
Contact book.department@intechopen.com

Numbers displayed above are based on latest data collected.
For more information visit www.intechopen.com



Optimized Imaging Techniques to Detect and Screen the Stages of Retinopathy of Prematurity

S. Prabakar¹, K. Porkumaran², Parag K. Shah³ and V. Narendran⁴

¹*Department of Electrical and Electronics Engineering,*

²*Institute of Technology, Coimbatore,*

^{3,4}*Department of Paediatric Retina & Ocular Oncology,
Aravind Eye Hospitals, Coimbatore,*

India

1. Introduction

Retinopathy of prematurity (ROP) is an ocular disease of premature infants and it can cause blindness on high threshold stages (Early Treatment of Retinopathy of Prematurity [ETROP] study, 2003). It affects immature vasculature in the eyes of premature babies (Wittchow.K, 2003; Mounir Bashour et al., 2008). It can be mild with no visual defects, or it may become aggressive with new blood vessel formation (neovascularization) and progress to retinal detachment and blindness (International Committee for the Classification of Retinopathy of Prematurity [ICCRP], 2005). As smaller and younger babies are surviving, the incidence of ROP has increased (Gwenole Quellec et al., 2008; Benson Shu Yan Lam & Hong Yan, 2008). All babies who less than 1800g birth weight or younger than 32 weeks gestational age at birth are at risk of developing ROP.

In any neonatal intensive care unit (NICU), the timing of the first evaluation must be based on the gestational age at birth. (a) If the baby is born at 23-24 weeks' gestational age, the first eye examination should be performed at 27-28 weeks gestational age. (b) If the baby is born at or beyond 25-28 weeks' gestational age, the first examination should occur at the fourth to fifth week of life. (c) Beyond 29 weeks, the first eye examination should probably occur by fourth week life time of baby.

It is essential that those caring for premature infants know who is at risk of retinopathy of prematurity, when screening must begin and how often these infants need to be examined. It is also important to know when to treat those infants who develop severe retinopathy of prematurity and what long term follow-up is needed to manage other complications of retinopathy of prematurity (Shankar, P. M. 1986). The discrimination between normal retinal vessels and diseased vessels plays a vital role to detect the ROP as shown in Fig. 1. The ROP occurs when abnormal blood vessels develop at the edge of normal retinal blood vessel. The ophthalmologists who are trained in ROP have to study and analyze the Retcam images.

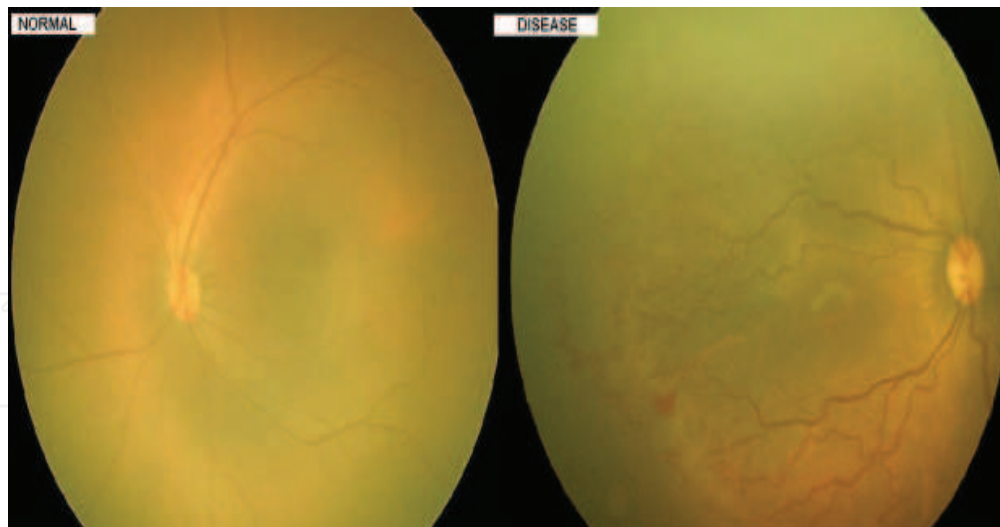


Fig. 1. Normal and Diseased Retinal Blood Vessels image of premature babies.

ROP is an ideal disease for applications and research in medical imaging for several reasons: (a) Clinical diagnosis is based solely on the appearance of disease in the retina. (b) There is a universally-accepted, evidence-based, diagnostic classification standard for ROP (ICCROP,2005). This ordinal system is used by ophthalmologists to define severe cases of ROP that require treatment, as well as cases with high-risk features that warrant particularly careful observation. (c) If severe ROP is diagnosed and treated early enough, blinding complications may be prevented. (d) ROP continues to be a leading cause of childhood blindness throughout the world. (e) Current ROP examination methods are time-intensive, frequently impractical, and physiologically stressful to premature infants. (f) Adequate ophthalmic expertise is often limited to larger ophthalmic centers, and therefore unavailable at the point of care. (g) Pilot studies have suggested that ROP diagnosis using simple interpretation of images captured using wide-angle digital retinal cameras may be feasible (Attar MA et al., 2005; Ells AL, Holmes JM, Astle WF, et al., 2003; Fierson WM, Palmer EA, Petersen RA, et al., 2001 ; Kaiser RS et al., 2001).

Indirect ophthalmoscope is the goal standard for ROP screening. But in a big way the indirect ophthalmoscope has been replaced with Retcam in ROP telescreening. Even though Retcam images can be taken by non ophthalmologist, it is difficult for them to interpret the stages of ROP. So, the proposed method giving a retinal image processing algorithm through which even a non ophthalmologist can give the various stages of ROP. This will provide the effective time utilization for the ophthalmologists. They can concentrate on infants who suffered with high risk threshold ROP and threshold ROP instead of analyzing all ROP images.

In this work, an automatic method is proposed to detect various stages of Retinopathy of prematurity (ROP) in premature infants and low birth weight infants. It is essential that those caring for premature infants should know who is at risk of ROP, when screening must begin and how often these infants need to be examined otherwise it can cause blindness. So, ROP detection is necessary for both screening the pathology and progression measurement. Computerizing this task, which is currently executed manually, would bring more subjectivity and reproducibility. The proposed image processing algorithms for predicting the presence and stages of ROP are histogram equalization methods, feature extraction, measuring curvature by changes in intensity and template matching. The retinal vessels are segmented using simple and standard 2-D Gaussian Matched Filter. Segmented vessels are thinned,

smoothened and filtered based on local intensity of the vessels. The classification of ROP stages has been implemented by trained and tested neural network's algorithms such as Back Propagation Feed Forward network (BPN), Radial Basis Function (RBF) network and the combination of both (Kai Chuan Chu & Dzulkifli Mohamad, 2003; Li Min Fu, 1994; Laurene Fausett, 1999; Meng Joo Er, shiqan wu, et al., 2002). The effectiveness of the proposed methods has been verified through machine vision techniques and the trained networks have been tested and validated with appropriate ROP input images. The results obtained are encouraged by experts and the data have been clearly discriminating the severity of ROP. Automatic ROP staging system comprises several advantages, like a substantial time reduction of ophthalmologists in diagnosis, a non ophthalmologist can provide stage of ROP, improving the sensitivity of the test and a better accuracy in diagnosis.

The following is the outline of the dissertation work presented in this paper:

Chapter 2 is devoted to the analysis and classification of ROP based on its severity. The common clinical procedure and diagnostic technique to detect the stage of ROP development in an infant has been discussed. Different images are provided for the illustration of the ROP localization and the feature extraction.

Chapter 3 deals with the development of generalized design of ROP classification and screening system. The design of proposed system model has been extended and a new combined model consists of Back Propagation Network (BPN) and Radial Basis Network (RBF).

In Chapter 4 and Chapter 5, various ROP image processing schemes such as image enhancement, fine classification, feature extraction, representation and ROP classification have been explained by different algorithms such as histogram equalisation technique, thresholding, averaging filter, median filter, edge detection and feature extraction. In the proposed neural network model, BPN network is combined with RBF network and the model outcomes have been compared and the computational details such as classification rate, and the time consumed by them have been evaluated and the results have been tabulated.

Chapter 6 is proposed to express the results and outcomes of various imaging techniques and neural network algorithms. The graphical representation and the tabulated values of extracted data provided the scope for the ROP screening. The results have been validated with experts and compared with common manual techniques for enhancement and future development and modifications

In chapter 7 proposed ROP image screening schemes and neural network classifiers are summarized together with suggestions for further research.

The acknowledgement and list of references which have been based on this work are given at the end chapters of this dissertation.

2. Retinopathy of prematurity (ROP)

Retinopathy of Prematurity (ROP) is a fibrovascular proliferative disorder, which affects the developing peripheral retinal vasculature of premature infants. It is an avoidable cause of blindness in children. The initial signs of ROP are detectable by a few weeks after birth, and the condition progresses rapidly thereafter. This means that screening has to be timely, and there is only a very narrow window of opportunity for treating. If not treated, the condition progresses rapidly to Stage 4 or 5 in approximately 50% of babies (Shah PK, Narendran V, et

al., 2009). The visual prognosis for babies with Stage 5 disease (total retinal detachment) is very poor, even after complex vitreoretinal surgery. The primary goal of screening is to detect all babies with treatable disease in time for treatment to be effective.

2.1 Classification of ROP

Blood vessel development in the retina occurs from the optic nerve out towards the periphery, that is, from the back of the eye towards the front. The location of the disease is referred by the ICROP (International Classification of Retinopathy of Prematurity) classification and is a measure of how far this normal progression of blood vessel development has progressed before the disease takes over (Mounir Bashour et al., 2008). Generally Zone II disease is more severe than Zone III disease and Zone I disease is the most dangerous of all since progression to extensive scar tissue formation and total retinal detachment is most likely in this location.

From the "flattened" retina shown in Fig. 2, we can see that:

- Zone I is a small area around the optic nerve and macula at the very back of the eye.
- Zone II extends from the edge of Zone I to the front of the retina on the nasal side of the eye (i.e. nose side) and part way to the front of the retina on the temporal side of the eye (i.e. temple side, or side of the head).
- Zone III is the remaining crescent of retina in front of Zone II on the temporal side of the eye.

Think of the eye as in time sections of a twelve hour clock to classify the stages of ROP. The extent of ROP is defined by how many clock hours of the eye's circumference are diseased. The numbers around the "flattened" retina in the Fig.2 shows the hours of the clock for each eye. For example, 3 o'clock is to the right, which is on the nasal side for the right eye and temporal side for the left eye. Often the disease is not present around all twelve clock hours, so a description may often refer to "x" number of clock hours of disease (e.g. nine clock hours would mean that three quarters of the circumference of the retina is involved).

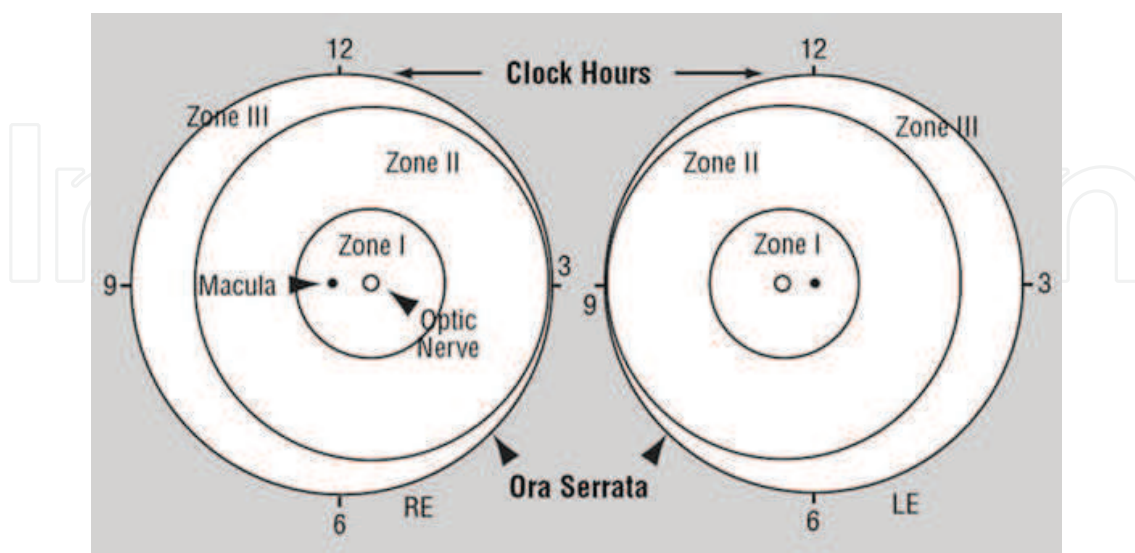


Fig. 2. Zone 1 is the most posterior retina that contains the optic nerve and the macula (zone of acute vision). Zone 2 is the intermediate zone where blood vessels often stop in ROP. Zone 3 is the peripheral zone of the retina, where vessels are absent in ROP, but present in normal eyes.

2.2 Stages of ROP based on ICROP

ROP is a rapidly progressive disease. It starts slowly, usually anywhere from the fourth to the tenth week of life, and may progress through successive stages, from Stage 1 to Stage 5, or it may stop at Stage 1 or Stage 2 or mild Stage 3 and disappear completely. The common ROP stage classification is shown in Table 1.

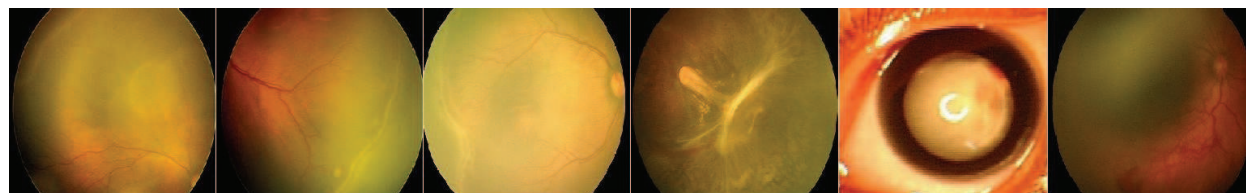


Fig. 3. Sequence of ROP Images visualizes Stage 1, Stage 2, Stage 3, Stage 4, Stage 5 and Plus Disease.

Stage 1. Demarcation line: a flat, white, thin line that separates the avascular retina anteriorly (toward the retinal periphery) from the vascularized retina posteriorly.

Stage 2. Ridge the flat line from stage 1 has grown in height, width, and volume and has become a pink-white ridge.

Stage 3. Ridge with extraretinal fibrovascular proliferation: proliferating tissue can be continuous with the posterior aspect of the ridge; immediately posterior to the ridge, or extending directly into the vitreous.

Stage 4. Subtotal retinal detachment: dragging vessels and subtotal traction retinal detachment can be seen. Stage 4A disease does not affect the macula and has a relatively good prognosis for vision; stage 4B disease affects the fovea and usually has a poor prognosis for vision.

Stage 5. Total retinal detachment: funnel-shaped retinal detachment. Anterior and posterior portions appear open or narrowed on ultrasonographic scans.

Plus Disease. The designation “+” is placed after the stage when dilated posterior veins, tortuous retinal arteries, vitreous haze, and pupillary rigidity are observed. If plus disease is observed in the posterior portion of the retina, patients must be monitored closely, as there is high risk of ROP progressing rapidly within a few days and lead to retinal detachment and may cause blindness with high risk ROP.

Category	Definitions
Stage 1	Demarcation line separating the avascular retina anteriorly from the vascularized retina posteriorly, with abnormal branching of small vessels immediately posterior.
Stage 2	Intra retinal ridge; the demarcation line has increased in volume, but this proliferative tissue remains intraretinal.
Stage 3	Ridge with extra retinal fibrovascular proliferation.
Stage 4	Partial retinal detachment.
Stage 5	Total retinal detachment.
Plus Disease	Two or more quadrants of vessel tortuosity and fullness at the optic nerve

Table 1. Definitions of ROP Severity Categories

2.3 Diagnosis of ROP

ROP is diagnosed from dilated ophthalmoscopic examination by an experienced ophthalmologist, and there are accepted guidelines for identifying high-risk premature infants who need serial screening examinations. Each image set consisted of 1 to 7 photographs from a single eye. Because imaging was performed at the bedside under typical working conditions, it was not possible to capture a standard set of photographs on each infant. The images have captured by Retcam for stage 1, stage 2, stage3, stage 4, stage 5 and Plus Disease as shown in Fig. 3.

Each infant underwent two examinations, which are sequentially performed under topical anaesthesia at the neonatal intensive care unit bedside: (a) Dilated ophthalmoscopy by an experienced ophthalmologist, based on well-known protocols (Kaiser RS et al., 2001; Fetus and Newborn Committee, Canadian Paediatric Society, 1998; Siatkowski RM & Flynn JT, 1998; Schaffer DB, Palmer EA, et al. 1993). The presence or absence of ROP disease, and its characteristics when present, were documented according to the international classification standard. (b) Wide-angle retinal imaging by an experienced ophthalmic photographer using a digital camera system (RetCam-120; MLI Inc., Pleasanton, California), based on guidelines established by the manufacturer.

The examinations are usually performed in the neonatal intensive care nursery where the neonatal staff can continue to monitor the baby. The infant will continue to be examined every 1 to 2 weeks until one of the following occurs:

- Development of the normal blood supply to the retina is complete.
- Two successive 2-week exams show Stage 2 in Zone III. Infants will then be examined every 4 to 6 weeks until the blood supply to the retina is fully developed.
- ROP is at "low risk prethreshold", just prior to requiring treatment. Follow-up exams will then occur every week until either "high risk prethreshold ROP or Threshold ROP" occurs, which requires treatment, or the retinopathy of prematurity disappears.
- The ROP is disappearing.

After two successive 2-week exams have shown regression, examinations should be continued every 4 to 6 weeks. Once the normal blood supply to the retina is completely developed, the infant will continue to be examined every 6 to 12 months by a pediatric ophthalmologist to ensure that no further complications of ROP occur.

3. Materials and methods

3.1 General design

Screening for ROP usually begins when the infant is about 4 to 6 weeks of age. An eye doctor (ophthalmologist), who specializes in either retinal disorders (retinal specialist) or children's eye diseases (pediatric ophthalmologist), uses a special instrument (an indirect ophthalmoscope) which allows a view through its optic lens into the back of the eye to examine the retina and determine whether development of the blood vessels is occurring normally or not. Before acquiring the retina images through Retcam, the infant is usually given some eye drops to make the pupil dilate so that the viewing field is as wide as possible. A light anaesthetic, in the form of numbing eye drops, may also be administered.

The general ROP screening system's flow diagram of the overall process as shown in Fig. 4, beginning with retinal image acquisition from the patient through Retcam. This image has been enhanced and removes the unwanted noise to obtain the object of interest. The required ROP features have been extracted by segmentation techniques and represent the image to train the machine to display that the severity of ROP. The error eradication system has been developed to obtain the better result. The decision making and classification modules used to provide the ROP presence and its stage. Normally the Stage 4 and Stage 5 ROP could not be treated. So, the present developed scheme has concentrated only on first three stages of the disease and Plus disease prognosis of ROP. Automatic ROP stage screening system will entail several advantages, like a substantial reduction in the labour workload of clinicians, improving the sensitivity of the test and a better accuracy in diagnosis by increasing the number of images.

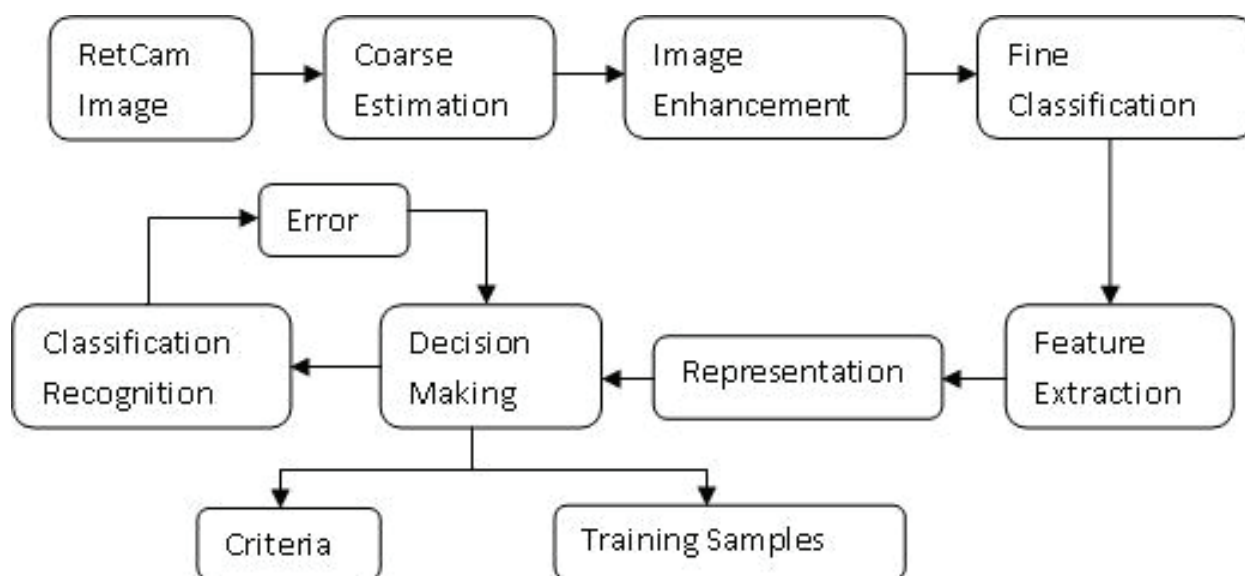


Fig. 4. Block diagram of the ROP detection and screening system.

The aim of this dissertation work is to design and develop an efficient ROP stage screening system. The main objectives of this work are as given below.

- To design a ROP image localizer to localize the region of interest from the image. ROP image localizer is used for segmenting the required blood vessels region from the input image.
- To develop a feature extractor for extracting the required classification features. Feature extractor is applied for getting the local features such as dilated vessels.
- To design a proper recognizer for recognizing the given image, Back Propagation network, Combination of BPN and RBF are to be developed for screening and recognition.

3.2 Proposed system model

Based on the general block diagram, the proposed system is designed. The model of the proposed system is given in Fig. 5.

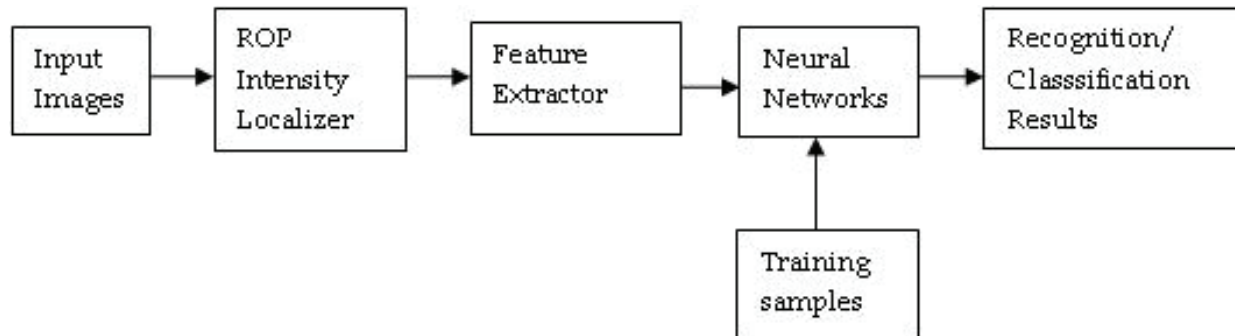


Fig. 5. Architecture of the proposed ROP classification and recognition system.

First, various pre-processing activities have been performed on the image for improving the quality of the image. These activities include image resizing, contrast stretching, histogram equalization and so on. The method of locating region of interest and dilated blood vessels are known as ROP image localization. Then, the local features such as abnormal branching of small vessels, Intra retinal ridge, ridge with extra retinal fibrovascular proliferation and partial and total retinal detachments are extracted from the region of interest. These values are given as the inputs to the neural networks for classification and recognition. Neural networks are trained with a set of training samples (Li Min Fu, 1994 ; Laurene Fausett, 1999 ; Meng Joo Er, shiqan wu, et al., 2002). The input images are compared with the trained samples and the similarity measures have been given as the classification and screening result. In this paper, Back Propagation Network (BPN), BPN + Radial Basis Function network (RBF) are used for classifying the ROP input images.

In the next section, we discover the appropriate machine vision techniques to detect the various stages ROP and the efficient neural network to classify and recognize the various ROP stages. The discussion begins with ideal model and to train the machine to identify the problem based on the requirements of the clinicians.

4. ROP image processing schemes

4.1 Proposed ROP image localization technique

ROP image localizer is designed to serve as a pre-processor of ROP stage classification and recognition systems for detecting the stage of ROP. The first step in this ROP image processing system is detecting the locations of blood vessels in the Retcam images. ROP image localization aims to localize the region of interest from the input image where blood vessels have been presented. Here the regions of interests are segmented and the regions that contain dilated, twisted and tortuosity of blood vessels. Various pre-processing activities are done in this stage to make the raw data into usable format.

A new algorithm is proposed in this proposal for localizing the ROP images, which consists of the following steps.

1. The input image is converted into the gray scale image.
2. The gray scale image is converted into its binary form.
3. The dilation operation is performed on the binary image. The dilation process removes the noise encountered in the binary image.

4. The dilated image is mapped on to the gray scale image.

Let I_m denotes the intensity of mapped image
 I_d denotes the intensity of the dilated image and
 I_g denotes the intensity of the gray scale image.

$$I_m(i, j) = \begin{cases} I_g(i, j) & \text{if } I_d(i, j) = 1 \\ \text{Otherwise} & \end{cases}$$

5. The mapped image has been converted into its binary form.
6. The required ROP region has been cropped from the binary image.

For developing a reliable ROP stage screening system, several ROP image processing activities have to be done. In this paper, the region on interest has been localized i.e., the required tortuosity and dilated vessels have been selected from the given input image using the proposed ROP localization technique. Instead of giving the whole image as input, the localized ROP image alone be given as input to the feature extractor and it diminishes the computational burden. A new algorithm is proposed in this work for extracting the local features and these features alone given as inputs to the neural network recognizer and classifier. This algorithm reduces the number of inputs to the recognizer as well as the training time.

4.2 Histogram equalization approach

First, it is necessary to describe the brightness variation in an image using its histogram. Then look at operations which manipulate the image so as to change the histogram, processes that shift and scale the result by making the image brighter or dimmer, in different ways. The intensity histogram shows how individual brightness levels are occupied in an image; the image contrast is measured by the range of brightness levels.

Histogram equalization is a non-linear process aimed to highlight image brightness in a way particularly suited to human visual analysis (Russ J. C., 1995; Jia X. & Nixon M. S. 1995; Baxes G. A., 1994; Parker J. R., 1994). Histogram equalization aims to change a picture in such a way as to produce a picture with a flatter histogram, where all levels are equiprobable. In order to develop the operator, it is important to inspect the histograms as shown in Fig. 6.

For a range of M levels, the histogram plots the points per level against level. For the input (old) and the output (new) image, the number of points per level is denoted as $O(l)$ and $N(l)$ (for $0 < l < M$), respectively. For square images, there are N^2 points in the input and the output image, so the sum of points per level in each should be equal:

$$\sum_{l=0}^M O(l) = \sum_{l=0}^M N(l) \tag{1}$$

Also, this should be the same for an arbitrarily chosen level p , since the aim is for an output picture with a uniformly flat histogram. So the cumulative histogram up to level p should be transformed to cover up to the level q in the new histogram:

$$\sum_{l=0}^p O(l) = \sum_{l=0}^p N(l) \quad (2)$$

Since the output histogram is uniformly flat, the cumulative histogram up to level p should be a fraction of the overall sum. So the number of points per level in the output picture is the ratio of the number of points to the range of levels in the output image:

$$N(l) = \frac{N^2}{N_{\max} - N_{\min}} \quad (3)$$

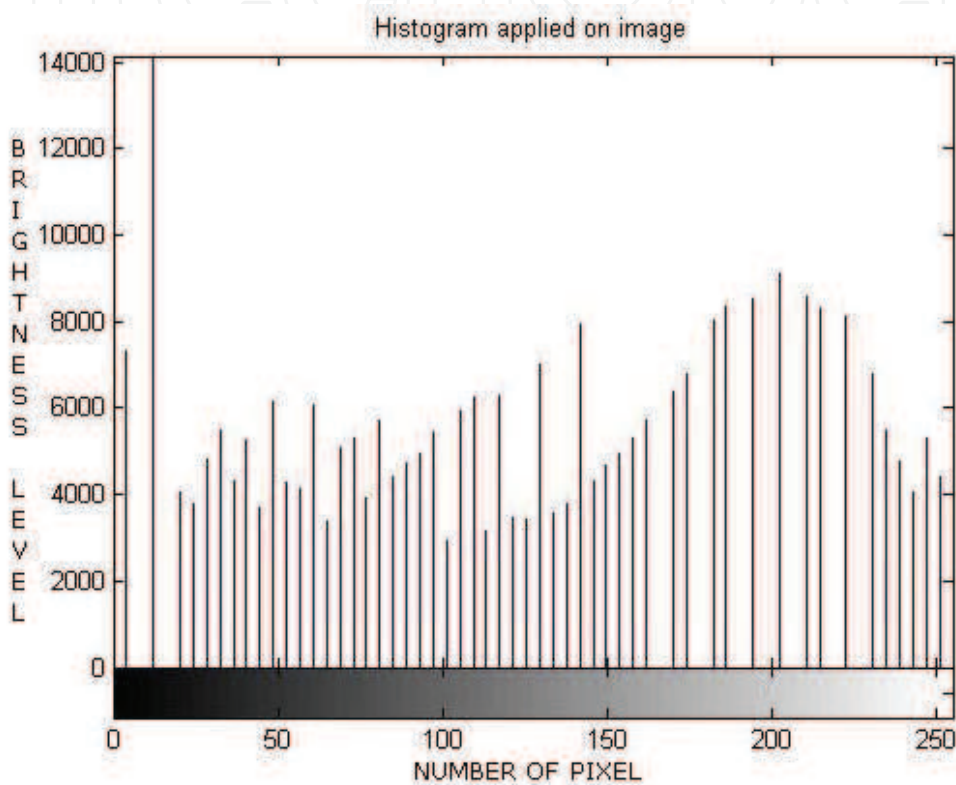


Fig. 6. Resulting Histogram applied on ROP image for enhancement.

So the cumulative histogram of the output picture is:

$$\sum_{l=0}^p N(l) = q \times \frac{N^2}{N_{\max} - N_{\min}} \quad (4)$$

Equation (2) shows that it is equal to the cumulative histogram of the input image, so:

$$q \times \frac{N^2}{N_{\max} - N_{\min}} = \sum_{l=0}^p O(l) \quad (5)$$

This gives a mapping for the output pixels at level q , from the input pixels at level p as:

$$q = \frac{N_{\max} - N_{\min}}{N^2} \times \sum_{l=0}^p O(l) \quad (6)$$

This gives a mapping function that provides an output image that has an approximately flat histogram. The mapping function is given by phrasing (6) as an equalizing function i.e., E of the level (q) and the image (O) as

$$E(q, O) = \sum_{l=0}^p O(l) = \sum_{l=0}^p N(l) \quad (7)$$

The output image is then

$$N_{x,y} = E(O_{x,y}, O) \quad (8)$$

The intensity equalized image has much better defined features than in the original version. The histogram reveals the non-linear mapping process whereby white and black are not assigned equal weight. Accordingly, more pixels are mapped into the darker region and the brighter intensities become better spread, consistent with the aims of histogram equalization. Its performance can be very convincing for ROP image, since it is well mapped to the properties of human vision.

4.3 Thresholding

There are more advanced techniques, known as optimal thresholding. These usually seek to select a value for the threshold that separates an object from its background. This suggests that the object has a different range of intensities to the background, in order that an appropriate threshold can be chosen.

Otsu's method (Sahoo P. K., Soltani S., Wong, A. K. C. et al., 1988) is one of the most popular techniques of optimal thresholding; applied for fine classification of ROP. Essentially, this technique maximizes the likelihood that the threshold is chosen so as to split the image between an object and its background. This is achieved by selecting a threshold that gives the best separation of classes, for all pixels in an image.

4.4 Averaging filter

For an averaging operator, the template weighting functions are unity. The template for an 7×7 averaging operator is implemented for the image. The result of averaging the ROP image with an 7×7 operator shows much of the details of the broad image structure.

The effect of averaging is to reduce noise, this is its advantage. An associated disadvantage is that averaging causes blurring which reduces detail in an image. It is also a low-pass filter since its effect is to allow low spatial frequencies to be retained, and to suppress high frequency components (Parker J. R., 1994; A.C. Bovik, T.S.Huang, & D.C.Munson, 1983). The size of an averaging operator is then equivalent to the reciprocal of the bandwidth of a low-pass filter it implements.

The averaging process is actually a statistical operator since it aims to estimate the mean of a local neighbourhood. The error in the process is naturally high, for a population of N samples; the statistical error is of the order of:

$$\text{error} = \frac{\text{mean}}{\sqrt{N}} \quad (9)$$

Increasing the averaging operator's size improves the error in the estimate of the mean, but at the expense of fine detail in the image. The average is of course an estimate optimal for a signal corrupted by additive Gaussian noise. The estimate of the mean maximized the probability that the noise has its mean value, namely zero.

According to the central limit theorem, the result of adding many noise sources together are a Gaussian distributed noise source. By the central limit theorem, the image noise can be assumed to be Gaussian. In fact, image noise is not necessarily Gaussian-distributed, giving rise to more statistical operators. It provides better pre-processing in ROP images and offers coarse estimation for the features.

4.5 Gaussian averaging filter

The Gaussian averaging operator has been considered to be optimal for image smoothing. The template for the Gaussian operator has values set by the Gaussian relationship. Let the x, y are the ROP image intensity values measured in both the (x, y) coordinates. The Gaussian functions 'g' at co-ordinates (x, y) is controlled by the variance ' σ^2 ' according to:

$$g(x, y) = e^{-\left(\frac{x^2 + y^2}{2\sigma^2}\right)} \quad (10)$$

Where, $g(x, y)$ gives a way to calculate coefficients for a Gaussian template which is then convolved with an image. It is clear that the Gaussian filter can offer improved performance compared with direct averaging: more features are retained whilst the noise is removed. This can lead to better performance in ROP images, since the contributions of the frequency components reduce in a controlled manner.

4.6 Median filter

The median is another frequently used statistic; the median is the centre of a rank-ordered distribution. The median is usually taken from a template centered on the point of interest. The median is the central component of the sorted vector (A.C. Bovik, T.S.Huang, & D.C. Munson, 1983).

The median operator is usually implemented using a template; here a 7×7 template is considered for ROP images. Accordingly, the system process the forty nine pixels in a template centered on a point with co-ordinates (x, y) . The median is the central component of the sorted vector; this is the twenty fifth component since we have forty nine values.

The median can of course be taken from larger template sizes. It is available as the median operator in Mathcad, but only for square matrices. The rank ordering process is computationally demanding slow and this has been motivated the use of template shapes other than a square. Common alternative shapes include a cross or a line (horizontal or vertical), centered on the point of interest, which can afford much faster operation since they cover fewer pixels.

The median filter has a well-known ability to remove salt and pepper noise. This form of noise, arising from, say, decoding errors in picture transmission systems, can cause isolated white and black points to appear within an image shown in Fig.6. When a median operator

is applied, the salt and pepper noise points will appear at either end of the rank ordered list and are removed by the median process. The median operator has practical advantage, due to its ability to retain edges i.e. the boundaries of shapes in images whilst suppressing the noise contamination.

4.7 Edge detection and feature extraction

The edges and required features of the ROP image have been detected by the Marr-Hildreth approach and Spacek operator (Petrou M. & Kittler J., 1991).

4.7.1 Marr–Hildreth approach

This method uses Gaussian filtering. In principle, we require an image which is the second differential ∇^2 of a Gaussian operator $g(x,y)$ convolved with an image P . This convolution process can be separated as:

$$\begin{aligned} \nabla g(x,y) &= \frac{\partial g(x,y)}{\partial x} U_x + \frac{\partial g(x,y)}{\partial y} U_y \\ &= -\frac{x}{\sigma^2} e^{-\frac{(x^2+y^2)}{2\sigma^2}} U_x - \frac{y}{\sigma^2} e^{-\frac{(x^2+y^2)}{2\sigma^2}} U_y \end{aligned} \tag{11}$$

$$\nabla^2(g(x,y) * P) = \nabla^2 g((x,y)) * P \tag{12}$$

Accordingly, we need to compute a template for $\nabla^2(g(x,y))$ and convolve this with the image. By further differentiation of (11), we achieve a Laplacian of Gaussian (LoG) operator:

$$\begin{aligned} \nabla^2 g(x,y) &= \frac{\partial^2 g(x,y)}{\partial x^2} U_x + \frac{\partial^2 g(x,y)}{\partial y^2} U_y \\ &= \frac{\partial \nabla g(x,y)}{\partial x} U_x + \frac{\partial \nabla g(x,y)}{\partial y} U_y \\ &= \left(\frac{x^2}{\sigma^2} - 1 \right) \frac{e^{-\frac{(x^2+y^2)}{2\sigma^2}}}{\sigma^2} + \left(\frac{y^2}{\sigma^2} - 1 \right) \frac{e^{-\frac{(x^2+y^2)}{2\sigma^2}}}{\sigma^2} \\ &= \frac{1}{\sigma^2} \left(\frac{x^2 + y^2}{\sigma^2} - 2 \right) e^{-\frac{(x^2+y^2)}{2\sigma^2}} \end{aligned} \tag{13}$$

This is the basis of the Marr-Hildreth operator. Equation (13) can be used to calculate the coefficients of a template which, when convolved with an image, combines Gaussian smoothing with second-order differentiation. It has been implemented to calculate template coefficients for the LoG operator, the function includes a normalization function, which ensures that the sum of the template coefficients is unity, so that the edges in the images are not clearly detected in area of uniform brightness. This is in contrast with the Laplacian operator (where the template coefficients summed to zero) since the LoG operator includes

smoothing within the differencing action, whereas the Laplacian is pure differencing. The Gaussian operator again suppresses the influence of points away from the centre of the template, basing differentiation on those points nearer the centre; the standard deviation, σ is chosen to ensure this action. Again, it is isotropic consistent with Gaussian smoothing. Determining the zero-crossing points is a major difficulty with this approach.

4.7.2 Spacek operator

Canny derived an operator to satisfy performance measures describing maximum signal to noise ratio and with good localization and chose a filter functional which maximized a composite measure of these parameters, whilst maintaining the suppression of false maxima (Trichili H et al., 2002). Essentially, whilst Canny maximized the ratio of the signal to noise ratio with the localization, Spacek maximized the ratio of the product of the signal to noise ratio and the peak separation with the localization. In Spacek's work, since the edge was again modeled as a step function, the ideal filter appeared to be of the same form as Canny's (Petrou M. & Kittler J, 1991). After simplification, this resulted in a one-dimensional optimal noise smoothing filter given by:

$$f(r) = (c_1 \sin(r) + c_2 \cos(r))e^r + (c_3 \sin(r) + c_4 \cos(r))e^{-r} + 1 \quad (14)$$

By numerical solution, Spacek determined optimal values for the constants as: $c_1 = 13.3816$, $c_2 = 2.7953$, $c_3 = 0.0542$ and $c_4 = -3.7953$. Spacek also showed how it was possible to derive operators which optimize filter performance for different combinations of the performance factors. In particular, an operator with the best possible noise suppression formulated by optimizing the noise suppression performance alone, without the other two measures, is given by:

$$f_c(r) = \frac{2 \sin(\pi r)}{\pi} - \cos(\pi r) + 2r + 1 \quad (15)$$

Spacek then showed how these operators could give better performance than Canny's formulation, as such challenging the optimality of the Gaussian operator for noise smoothing (in step edge detection) (Petrou M. & Kittler J, 1988). In application, such an advantage has been produced better output of ROP image. This is the vital feature used to detect the plus disease of ROP.

One difficulty with optimal smoothing functional expressed in one-dimensional form is their extension to become a two-dimensional image operator. For the Spacek operator, one approach is to consider (14) as a circularly symmetric functional expressed in terms of radius 'r' and to generate the coefficients of a template smoothing operator in this manner.

4.8 Image curvature detection

Edges are perhaps the low-level image features that are most obvious to human vision. They preserve significant features, so they can be usually recognized what an image contains from its edge-detected version. However, there are other low-level features that can be used in computer vision. One important feature is curvature. Intuitively, it is important to consider curvature as the rate of change in edge direction (Mokhtarian F. & Mackworth A. K., 1986). This rate of change characterizes the points in a curve; points where the edge

direction changes rapidly are corners, whereas points where there is little change in edge direction correspond to straight lines. Such extreme points are very useful for shape description and matching in ROP severity prediction, since they represent significant information with reduced data.

The main problem with this approach is that it depends on the extraction of sequences of pixels. In ROP images, it is very difficult to trace a digital curve in the image. This is because noise in the data can cause edges to be missed or to be found inaccurately. This problem may be handled by using a robust fitting technique. However, the implementation is not evident. By using this robust fitting for each image pixel, then the curvature could be computed as the inverse ratio of a circle.

5. Proposed ROP classification using neural networks

5.1 Proposed BPN and RBF classifier and recognizer model

After extracting the required ROP features from the Retcam images, a classifier and recognizer is needed to screen the severity of ROP. Neural Networks can be applied for such problems to classify and recognize through the training and testing of samples. In this chapter Back Propagation Network (BPN) and a combined model of BPN and Radial Basis Function (RBF) network are proposed as classifiers and recognizers.

5.2 Back propagation network (BPN)

Back Propagation Network (BPN) can train multi layer feed-forward networks with differentiable transfer functions to perform function approximation, pattern association, and pattern classification (Laurene Fausett et al., 1999; Li Min Fu, 1994).

The BPN is designed in this work with one input layer, one hidden layer and one output layer. The input layer consists of six neurons. The inputs to this network are feature vectors derived by applying the image processing calculations and algorithms. The network is trained using the features extracted from processed Retcam ROP images.

The Back propagation training takes place in three stages:

1. Feed forward of input training pattern
2. Back Propagation of the associated error and
3. Weight adjustment

During feed forward, each input neuron receives an input value and broadcasts it to each hidden neuron, which in turn computes the activation and passes it on to each output unit, which again computes the activation to obtain the net output. During training, the net output is compared with the target value and the appropriate error is calculated. From this, the error factor is obtained which is used to distribute the error back to the hidden layer. The weights are updated accordingly. In a similar manner, the error factor is calculated for hidden units. After the error factors are obtained, the weights are updated simultaneously. The output layer contains one neuron. The result from the output layer is considered as the recognition result. The gradient descent algorithm which has been utilized in BPN is generally very slow because it requires small learning rates for stable learning. In order to avoid this, BPN is combined with Radial Basis Function Network.

5.3 Combined framework of BPN and RBF

Radial Basis Function (RBF) neural networks have recently attracted extensive research works because of their best approximation property, very compact topology and universal approximators and also their learning speed is very fast because of local-tuned neurons. RBF networks are used for function approximation (Meng Joo Er, shiqan wu, Juwei Lu, et al., 2002). In this paper, a RBF neural network is used as classifier and recognizer in the ROP screening system and the inputs to this network are the results obtained from the BPN. So, the result obtained from the output layer of BPN is given as the input to the RBF. RBF uses the gaussian function for approximation. For approximating the output of BPN, it is connected with RBF.

The RBF neural network has a feed forward architecture with an input layer, a hidden layer and an output layer. Fig. 7 shows the combined framework of BPN and RBF.

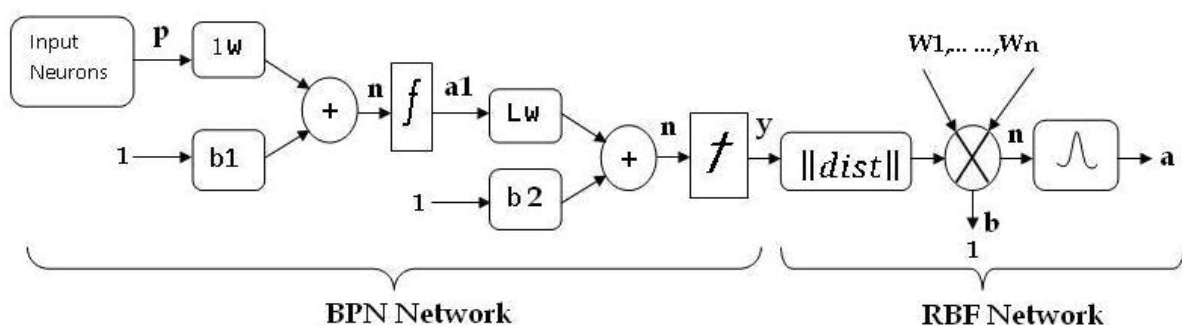


Fig. 7. Combined Framework of BPN and RBF.

$$a1 = \text{tansig}(IW * p + b)$$

$$y = \text{purelin}(LW * a + b) \quad a = \text{radbas}(\|w - p\| / b)$$

where

$$a1 = \text{tansig}(IW * p + LW + b1)$$

$$y = \text{purelin}(LW * a1 + b2)$$

$$a = \text{radbas}(\|w - p\| / b)$$

$$p = \text{Set of input neurons}$$

$$b1 = \text{bias to the input layer}$$

$$b2 = \text{bias to the hidden layer}$$

$$b = \text{bias to the RBF neuron}$$

$$IW = \text{Weight between Input and hidden layers}$$

$$LW = \text{Weight between hidden and Output layers}$$

$$y = \text{Output of BPN}$$

$$Wi = \text{Weight vector to RBF}$$

$$a = \text{RBF output}$$

The RBF network is simulated by giving the output of BPN as input to RBF.

6. Results and discussion

The automatic ROP severity identification methodologies have been developed and implemented to analyze the various infant's ROP images with different stages such as stage1, stage 2, and stage 3. Since, the stage 4 and stage 5 are highly critical and almost the retina has been detached as shown in Fig. 2, the images of these stages have not been

considered for our present analysis and prediction and also these stages will not provide fruitful improvement in the vision system on treatment. All the images have been taken by Retcam and are available either in .bmp or .jpeg format with 640X480 sizes. The specific image enhancement and smoothing are obtained by the histogram approach and various filtering techniques such as averaging and median filter methods. The ROP image localizer and other image processing techniques have been implemented and the corresponding results for every stage have been obtained as shown in Fig. 8. The feature extraction and segmentation of the ROP images have been estimated by applying various operators and the exact stage could be identified by the curvature detection approach as shown in Fig. 9.

Detecting pathological retina images in premature infants is a challenging problem. In the proposed methods, the various ROP severities have been identified properly by providing the images to the neural network classifier and recognizer. The results in Table 2 show that our method is able to yield an accurate result and is appreciated by experts. The ROP intensity levels have been extracted in the images taken from various patients with appropriate time interval in terms of prognosis weeks. The ROP diagnosis and treatment are the continuous procedure and will extend minimum for a period of six months. Table 2 shows the four weeks diagnosis of ROP images with various severities in various cases.

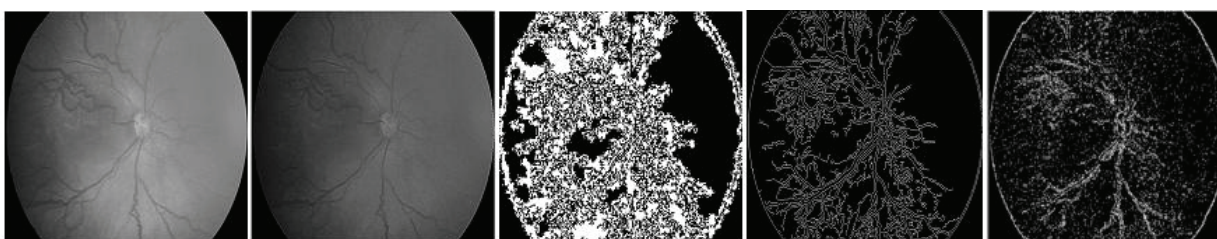


Fig. 8. Processed gray scale images of stage 3 and plus diseased ROP, Image smoothed by Median filter, Binary filled holes, Canny Filtered Image, Dilated Gradient Mask

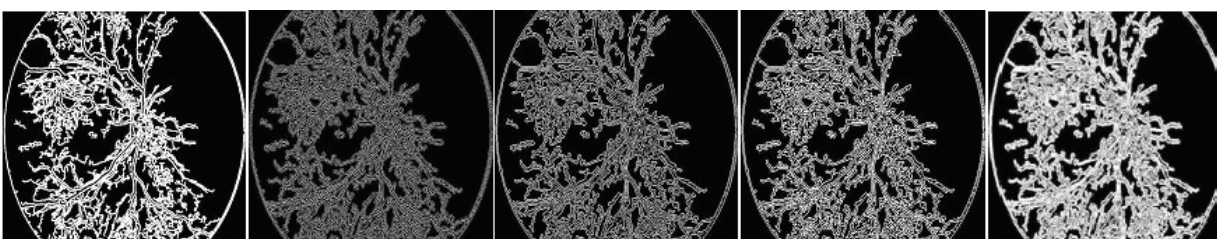


Fig. 9. Processed ROP images such as Dilated Image, Eroded Image, Average Filtered Image, Median Filtered Image, and Segmented Image

For the methodologies application, from each case we have considered 10 to 15 images of various locations of retinal portion and blood vessels development. Initial four weeks of ROP images have been deemed and the averaged ROP intensity level has been calculated by a mixture of image processing algorithms. The ROP images have been acquired for every case with corresponding time interval. Follow-up exams will then occur every week until either high risk prethreshold ROP or threshold ROP occurs, which requires treatment, or procedure continues till the ROP disappears.

The severity of ROP prognosis in various cases with appropriate time duration has been shown in Fig. 10. The proposed method detects the stage 1, Stage 2, stage 3 and plus disease ROP intensity levels and the result has been appraised by the ophthalmologists. Based on

the analysis the treatment could be started and further follow-up examinations could be taken place in every week.

The effectiveness of the proposed ROP localization technique and the ROP severity screening algorithm are demonstrated using the computer simulations. The processed ROP image database consists of 130 images for 13 different cases of infants. Out of 130 images, 65 images have been taken for training the BPN and RBF networks. The training database has been stored for feature reference and further differentiation. The fine classification of various stages of ROP based on the severity could be acquired by modifying the stored features of various stages of ROP images. This is the very useful feature of automatic stage screening system using neural network. The number of epochs versus the squared error graph is shown in the Fig. 11.

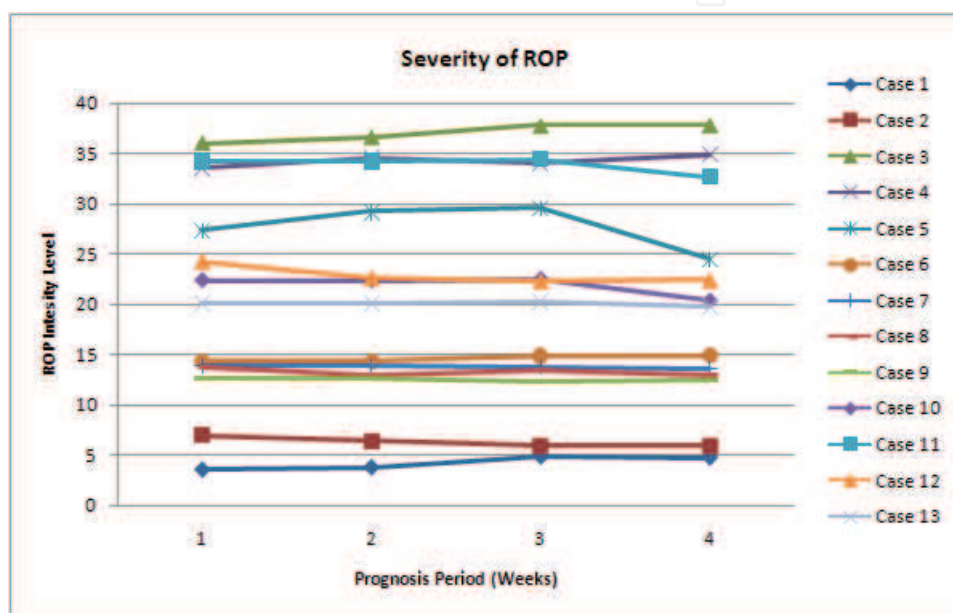


Fig. 10. Severity of ROP intensity distribution for different cases

Severity of ROP	Case	Prognosis Period in Weeks			
		1	2	3	4
Stage 1	1	3.58587	3.81205	4.82632	4.72649
	2	6.97861	6.39284	5.93572	5.92018
Stage 2	3	36.03182	36.61781	37.76183	37.82493
	4	33.52674	34.56846	34.01264	34.92073
	5	27.42039	29.21654	29.56214	24.54281
Stage 3	6	14.33021	14.3312	14.87012	14.88023
	7	13.86317	13.86245	13.78453	13.65245
	8	13.78317	12.89521	13.35481	12.8729
	9	12.62624	12.62434	12.34675	12.4392
	10	22.36995	22.33591	22.45786	20.38219
Plus Disease	11	34.22109	34.22109	34.45215	32.69103
	12	24.28109	22.62306	22.26518	22.35671
	13	20.10566	20.10566	20.24308	19.73859

Table 2. Severity of ROP for various cases in proper time interval.

Then the Neural Networks are tested with the remaining various stages of ROP images. The BPN network predicts 3 cases indistinctly and provides erroneous classification for Stage2, Stage 4 and Stage 5. The combined model of BPN+RBF classifies and recognizes all the ROP images with proper stage classification except stage 2. The time consumption and the classification and recognition rate are tabulated in Table 3.

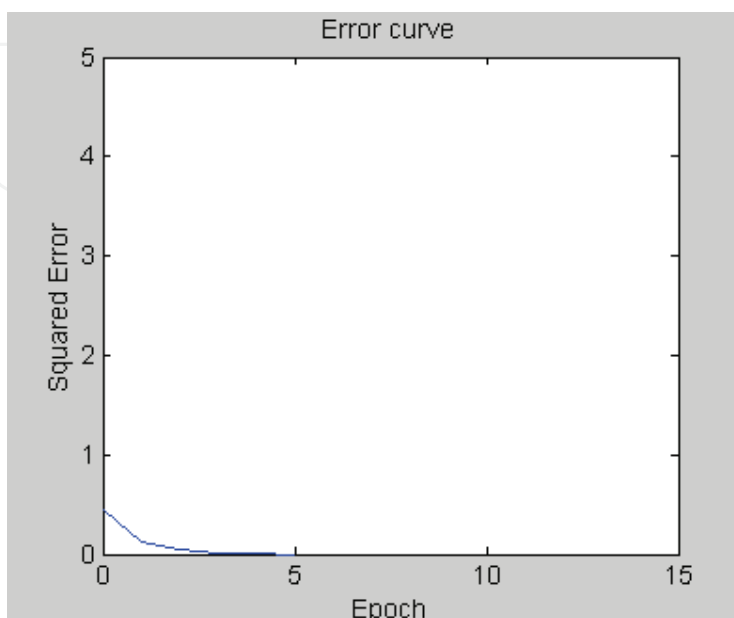


Fig. 11. Error rate versus number of Epochs (BPN Training)

Network	Training+ Testing time (in seconds)	Recognition Rate (in %)
BPN	15.5490	98.4
BPN+RBF	15.5640	99.2

Table 3. Comparison of BPN+RBF framework over BPN.

The false positive and the false negative rates of BPN and BPN+RBF networks are listed in Table 4.

Network	Number of Images	False Classification	False Dismissal
BPN	130	3	0
BPN+RBF	130	1	0

Table 4. Results of the proposed method over the whole test set (BPN and BPN+RBF).

From this result, the proposed model of combined BPN and RBF network has delivered better ROP classifiers and recognizers. The outcomes of this hybrid model have been evaluated by the experts and which may provide the best analysis of ROP severity. ROP severity screening depicts that some stages have rapid difference in its intensity levels in time duration and some have negligible levels of variation in its prognosis. Any how based on the intensity level, classification and recognition the physician could reach up a solution of the necessary method and time period to treat the disease. Then the treatment will reduce the prognosis of the disease and has to be verified every time.

7. Conclusion

In this work, proper ROP screening system has been designed to carry out the classification and recognition of various severity and stages of ROP. Initially, Back Propagation Network (BPN) is used as the recognizer. The features extracted from the different image processing algorithms in Chapter 4 are given as the input to BPN. The implementation of zone fitting and further enhancement of ROP intensity level will produce predominant result. The method introduced here utilizes the well-known framework of commonly using imaging techniques which have provided the best ROP database for further processing such as classification and recognition. BPN is trained with a set of images and the weights are updated. After training, the features of the image has to be tested are given as input. The network is simulated using these input values and the result is obtained. The proposed method shows a good performance for stage 3 and plus disease images. The ratio of the number of images correctly identified the stage of ROP to the total number of images gives the recognition result.

To enhance the performance of BPN, it is combined with RBF. RBF network can approximate any type of function. The output obtained from BPN is given as the input to RBF. RBF is simulated using this input and the output is acquired which is considered to be the Classification and recognition result. From the simulation results, it can be observed that the recognition rate of the combined BPN and RBF model is considerably high. The effectiveness of the proposed method has been demonstrated through experimentation using various ROP diseased cases.

Still further improvement may be required for the precise classification and identification of stage 1 and stage 2. Since, it might be that the exact shape is unknown or it might be that the perturbation of that shape is impossible to parameterize (Huertas A. & Medioni G. 1986; Mokhtarian F. & Mackworth A. K. 1986; Committee for the Classification of Retinopathy of Prematurity, 1984 ; Cryotherapy for Retinopathy of Prematurity Cooperative Group, 1988). In these cases, we seek techniques that can evolve to the target solution, or adapt their result to the data. This implies the use of flexible shape formulations. The snake model could be used to identify the flexible formulations and the results of the same could be delivered to the neural network classifiers.

In future we can combine the proposed methods and different implementations of the snake model to detect the flexible patterns. The wavelet based image fusion technique may also be utilized to produce better result in stage 1 and stage 2 classes of images. The ROP concentration will further be categorized and identified with image registration and fusion techniques. The artificial neural network algorithms may also be enhanced by Adaptive Resonance Theory (ART1) network and the Learning Vector Quantization (LVQ) network to train the system to produce better result and automation of ROP diagnosis in a successful manner. This ROP stage classification recognition system will also satisfy the prediction of stage 4 and stage 5 with better accuracy. The Graphical User Interface (GUI) based menu options will provide user friendly environment for non ophthalmologist so that the time consumption of ophthalmologists can be considerably reduced i.e. instead of analyzing all Retcam images they provide prominent diagnosis on the infants who have suffered with severe stage ROP.

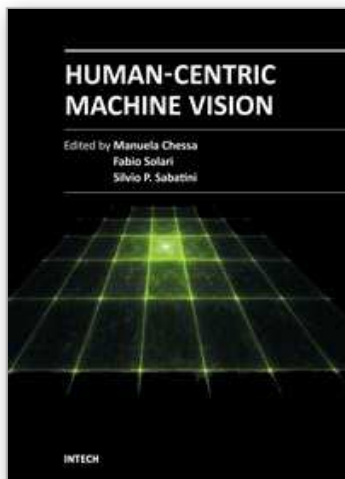
8. Acknowledgment

The authors would like to thank Dr. N.G.P. Institute of Technology, Kovai Medical Center Hospital, Coimbatore and Aravind eye hospital, Coimbatore for providing necessary facilities to carry out this work. The suggestions and comments of anonymous reviewers, which have greatly helped to improve the quality of this paper, are acknowledged.

9. References

- A.C. Bovik, T.S. Huang, and D.C. Munson, (1983) "A Generalization of Median Filtering using Linear Combinations of Order Statistics," *IEEE Transaction on Acoustics, Speech and Signal Processing*, vol. ASSp-31, no.6, pp.1342-1350
- Attar MA, Gates MR, Iatrow AM, Lang SW, Bratton SL. (2005) "Barriers to screening infants for retinopathy of prematurity after discharge or transfer from a neonatal intensive care unit," [PubMed: 15496873] *J Perinatol*, 25:36-40
- Baxes, G. A. (1994), "*Digital Image Processing, Principles and Applications*," Wiley & Sons Inc., NY USA
- Benson Shu Yan Lam and Hong Yan (2008) "A novel vessel segmentation algorithm for pathological retina images based on the divergence of vector fields," *IEEE Trans. Med. Imag.*, Vol.27, No.2, pp237-246
- Committee for the Classification of Retinopathy of Prematurity (1984) "An international classification of retinopathy of prematurity," *Arch Ophthalmol*; 102: 1130-4
- Cryotherapy for Retinopathy of Prematurity Cooperative Group (1988) "Multicenter trial of cryotherapy for retinopathy of prematurity. Preliminary results," *Arch Ophthalmol*; 106:471-9
- Early Treatment of Retinopathy of Prematurity Cooperative Group (2003). "Revised indications for the treatment of retinopathy of prematurity," *Arch Ophthalmol*; 121: 1684-96.
- Ells AL, Holmes JM, Astle WF, et al. (2003) Telemedicine approach to screening for severe retinopathy of prematurity: a pilot study. *Ophthalmology*; 110: 2113-7
- Fetus and Newborn Committee, Canadian Paediatric Society. (1998) "Retinopathy of prematurity: recommendations for screening," *Pediatric Child Health*; 3:197-8
- Fierson WM, Palmer EA, Petersen RA, et al. (2001) "Screening examination of premature infants for retinopathy of prematurity," *Pediatrics*; 108:809-11
- Gwenole Quellec, Mathieu Lamard, Pierre Marie Josselin & Guy Cazuguel (2008) "Optimal Wavelet transform for the Detection of Microaneurysms in Retina Photographs," *IEEE Trans. Med. Imag.*, vol.27, No.9, pp.1230-1241
- Huertas, A. and Medioni, G. (1986) "Detection of Intensity Changes with Subpixel Accuracy using Laplacian-Gaussian Masks," *IEEE Trans. on PAMI*, 8(1), pp. 651-664
- International Committee for the Classification of Retinopathy of Prematurity (2005) "The international classification of retinopathy of prematurity revisited," *Arch Ophthalmol*; 123:991-9
- Jia, X. and Nixon, M. S. (1995) "Extending the Feature Vector for Automatic Face Recognition," *IEEE Trans. on PAMI*, 17(12), pp. 1167-1176
- Kai Chuan Chu, and Dzulkifli Mohamad, (August 3-5, 2003) "Development of a Face Recognition System using Artificial Intelligent Techniques based on Hybrid

- Feature Selection, " Proc. Of the second Intl. Conference on Artificial Intelligence in Engineering and Technology, Malaysia, pp. 365-370
- Kaiser RS, Trese MT, Williams GA, Cox MS Jr. (2001) "Adult retinopathy of prematurity: outcomes of rhegmatogenous retinal detachments and retinal tears," *Ophthalmology*; 108:1647-53
- Lamdan, Y., Schawatz, J. and Wolfon, H. (1988) "Object Recognition by Affine Invariant Matching," *Proc. IEEE Conf. on Computer Vision and Pattern Recognition*, pp. 335-344.
- Laurene Fausett, (1999) "*Fundamentals of Neural Networks*," Prentice Hall, New Jersey
- Li Min Fu, (1994) "*Neural Networks in Computer Intelligence*," McGraw-Hill Inc., Singapore
- Loupas, T. and McDicken, W. N. (1987) "Noise Reduction in Ultrasound Images by Digital Filtering," *British Journal of Radiology*, 60, pp. 389-392
- Meng Joo Er, shiqan wu, Juwei Lu, and Hock Lye Toh, (May 2002) "Face Recognition with Radial Basis Function (RBF) Neural Networks," *IEEE Transactions on Neural Networks*, vol.13, No.3, pp.697-710
- Mokhtarian, F. and Mackworth, A. K. (1986) "A Theory of Multi-Scale, Curvature-Based Shape Representation for Planar Curves," *IEEE Trans. on PAMI*, 14(8), pp. 789-805
- Mounir Bashour, Johanne Menassa & C Cornia Gerontis (2008) "*Retinopathy of Prematurity*," Nov, [Online] Available: <http://www.emedicine.medscape.com/article/1225022>
- Palmer EA, Flynn JT, Hardy R. (1991) Incidence and early course of retinopathy of prematurity. *Ophthalmology*; 98:1628-40
- Parker, J. R. (1994), "*Practical Computer Vision using C*," Wiley & Sons Inc., NY USA
- Petrou, M. and Kittler, J.(1991) Optimal Edge Detectors for Ramp Edges, *IEEE Trans. on PAMI*, 13(5), pp. 483-491
- Petrou.M and Kittler.J (1988) "On the optimal edge detector," Proc. of The british Machine Vision Conference (BMVC) by BMVA, Alvey Vision Conference, pp 191- 196
- Russ, J. C. (1995) "*The Image Processing Handbook*," 2nd Edition, CRC Press (IEEE Press), Boca Raton, FL USA
- Sahoo, P. K., Soltani, S., Wong, A. K. C. and Chen, Y. C. (1988) "Survey of Thresholding Techniques," *CVGIP*, 41(2), pp. 233-260
- Schaffer DB, Palmer EA, Plotsky DF, Metz HS, Flynn JT, Tung B, et al. (1993) "Prognostic factors in the natural course of retinopathy of prematurity," *Ophthalmology*;100:230-7
- Shah PK, Narendran V, Kalpana N, Tawansy KA. (2009), "Anatomical and visual outcome of stages 4 and 5 retinopathy of prematurity," *Eye* 2009, 23:176-180
- Shankar, P. M. (1986) "Speckle Reduction in Ultrasound B Scans using Weighted Averaging in Spatial Compounding," *IEEE Trans. on Ultrasonics, Ferroelectrics and Frequency Control*, 33(6), pp. 754-758
- Siatkowski RM, Flynn JT. (1998) "*Retinopathy of Prematurity*. In Nelson L,ed. *Harely's Pediatric Ophthalmology*," 4th ed. Philadelphia: WB Saunders& Co.
- Trichili, H.; Bouhlel, M.-S.; Derbel, N.; Kamoun, L.; (6-9 Oct. 2002), "A survey and evaluation of edge detection operators application to medical images," Systems, Man and Cybernetics, 2002 IEEE International Conference on, vol.4, no., pp. 4
- Wittchow.K (2003) "Shared liability for ROP screening," *OMIC Journal*.P.3 <http://www.omic.com/new/digest/DigestFall03.pdf> accessed November 20, (2009)



Human-Centric Machine Vision

Edited by Dr. Fabio Solari

ISBN 978-953-51-0563-3

Hard cover, 180 pages

Publisher InTech

Published online 02, May, 2012

Published in print edition May, 2012

Recently, the algorithms for the processing of the visual information have greatly evolved, providing efficient and effective solutions to cope with the variability and the complexity of real-world environments. These achievements yield to the development of Machine Vision systems that overcome the typical industrial applications, where the environments are controlled and the tasks are very specific, towards the use of innovative solutions to face with everyday needs of people. The Human-Centric Machine Vision can help to solve the problems raised by the needs of our society, e.g. security and safety, health care, medical imaging, and human machine interface. In such applications it is necessary to handle changing, unpredictable and complex situations, and to take care of the presence of humans.

How to reference

In order to correctly reference this scholarly work, feel free to copy and paste the following:

S. Prabakar, K. Porkumaran, Parag K. Shah and V. Narendran (2012). Optimized Imaging Techniques to Detect and Screen the Stages of Retinopathy of Prematurity, Human-Centric Machine Vision, Dr. Fabio Solari (Ed.), ISBN: 978-953-51-0563-3, InTech, Available from: <http://www.intechopen.com/books/human-centric-machine-vision/optimized-imaging-techniques-to-detect-and-screen-the-stages-of-retinopathy-of-prematurity>

INTECH
open science | open minds

InTech Europe

University Campus STeP Ri
Slavka Krautzeka 83/A
51000 Rijeka, Croatia
Phone: +385 (51) 770 447
Fax: +385 (51) 686 166
www.intechopen.com

InTech China

Unit 405, Office Block, Hotel Equatorial Shanghai
No.65, Yan An Road (West), Shanghai, 200040, China
中国上海市延安西路65号上海国际贵都大饭店办公楼405单元
Phone: +86-21-62489820
Fax: +86-21-62489821

© 2012 The Author(s). Licensee IntechOpen. This is an open access article distributed under the terms of the [Creative Commons Attribution 3.0 License](#), which permits unrestricted use, distribution, and reproduction in any medium, provided the original work is properly cited.

IntechOpen

IntechOpen